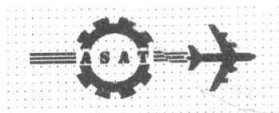


Military Technical College
Kobry El-Kobbah
Cairo, Egypt



10th International Conference
On Aerospace Sciences &
Aviation Technology

PERFORATION OF A SMALL CALIBER PROJECTILE INTO TEXTILE/EPOXY COMPOSITE TARGETS

BY

A. I. Fayed*, A. M. Riad* and S. A. Salah*

ABSTRACT

An experimental program has been conducted to study the normal perforation of a small caliber projectile into textile/epoxy composite targets. This program is concerned with the determination of ballistic resistance for a set of targets, consisting of kevlar/epoxy and S-2 glass/epoxy composites with different thicknesses. The used textiles (kevlar-129 and S-2 glass) for manufacturing the composites have a new weave shape (3D weaveTM), which permits the epoxy resin to diffuse through it. In addition, tensile tests of manufactured composite specimens are performed to determine their mechanical properties.

The analytical model developed by Taylor and Vinson [1] is adopted herein to describe the penetration of a small caliber projectile into a textile/epoxy composite target. The selected model uses the circumferential strain as a failure criterion for a composite target. The main assumptions and equations representing the analytical model are presented. These equations are arranged and compiled into a computer program. The input data to run the program are easily determined.

The ballistic measurements of the experimental program are compared with the model predictions; good agreement is generally obtained. The obtained results show that the tested composites with different thicknesses have a limited ballistic resistance against the used projectile. Moreover, other types of epoxies are recommended be used for manufacturing the composites and the effect of epoxy type as well as the delamination between composite layers on their ballistic resistance must be considered.

KEY WORDS: Composite mechanics, body armors, impact dynamics, penetration mechanics, and lightweight targets.

* Egyptian Armed Forces

INTRODUCTION

Nowadays, both para-aramides and polyethylene's acquire advanced position, in the field of ballistic impact, among the other metallic and non-metallic lightweight material systems [2]. Textile reinforced composites have been used as armor materials due to their lightweight, good energy absorbability and high specific strength. These composites are applied to the structure of modern armor fighting vehicles, body armors and other different applications.

Mohamed et al. [3] constructed a new fabric consisting of 3-D orthogonal weaving (3TEX 3 Weave™ process). They showed that the new weave process had great potential for low cost manufacturing of thick performs. The developed fabrics combined no-crimp in-plane fabric reinforcement with integral through thickness (z-direction) reinforcement. This reinforcement eliminated the delamination, and improved the interlaminar strength and damage tolerance of composite. Their new weave has great advantages in composites processing; it allowed the different types of epoxies to diffuse through them with penetration speed higher than that for the 2D fabric stacks. The new fabric construction of S-2 glass and/or kevlar 129 with, for example, epoxy vinyl ester, rubber-toughened epoxy, and some other epoxy products were used to build new composites for manufacturing body armors and light helmets.

Vinson and Zukas [4] developed a model determining the actual response of textile fabric panels subjected to ballistic impact by a dense projectile. They formulated stepwise procedures for calculating strains, projectile position, forces and decelerations as functions of penetration time. Their analytical results were in good agreement with experimental data due to the impact of a 5.6 mm projectile into 1 and 12 plies of nylon and 24 plies of kevlar-29 textile, respectively. Taylor and Vinson [1] extended the model of Ref. [4] by determining the material properties of a target and the geometry of a deflected cone at each time step, allowing a complete description of the impact event. They also performed ballistic tests by impacting 5.6 and 9 mm bullets against single and multi-layered Kevlar-29 fabrics, respectively, to assess their model predictions.

Zhu et al. [5] developed an analytical model describing the normal impact and perforation of a conical-tipped hard steel cylinder into kevlar-29/polyster composite laminates. They modeled the dissipative mechanisms including indentation of striker tip, bulging at the back surface, fiber failure, delamination and friction using simplified assumptions. They divided the impact event into three consecutive phases; these were indentation, perforation and exit phases. They also performed an experimental program in which they measured the ballistic limits and projectile velocity after perforating the tested laminates. Good agreement was obtained between their model predictions and experimental measurements.

Morye et al. [6] presented a semi-empirical model to simulate the ballistic impact of a 5 mm steel projectile into nylon-66 fibre composite targets at $V_i=512$ m/s. Their model predicted the effect of fibre modulus, fiber failure strain and energy absorbed in tensile failure of the fibre on the ballistic limit of the composite. The photographs of their experimental program showed a deformation cone due to the impact; complete penetration occurred when the cone radius reached a value of 13.8 mm and the projectile exit with a residual velocity of 191 m/s. Moreover, they found no evidence for fiber residual stretching, suggesting that the material was highly elastic and its failure always occurred after the elastic limit.

Sharma et al. [7] used a finite difference code, Autodyn-2D, to simulate the impact of a 1.1 g stainless steel projectile into four different targets materials, respectively. These materials were Polycarbonate, Ti-6%Al-4%V, Dyneema UD66 HBI composite and Ti-6%A1-4%V/Dyneema UD66 HBI hybrids. They investigated the post-failure examinations of different types of composites using ultrasonic C-scan optical microscopy. They deduced that the micro-mechanical mechanisms of failure could not be modeled by Autodyn-2D.

Shahkarami et al. [8] used a 3-D finite element code, named LS-Dyna, to simulate the ballistic response of soft, multi-layered, fabric materials employed in body armors. The code described the impact between projectile and fabric, and it ensured the interactions among the various layers of the fabric. Supporting experimental measurements were conducted to assess the validity of their numerical predictions.

Potti and Sun [9] used a so-called static punch curve as the 'structural constitutive model' to capture the highly non-linear behavior of a thick composite laminate during its penetration process. They used the ring element model to simulate the static punch curve. In addition, they modeled the dynamic penetration process of large panels using the data obtained from the static punch curve. Their model was capable of predicting the delaminated areas of targets with different thicknesses during their impact with different velocities. For each composite thickness, they deduced that the delaminated area increased with impact velocity until the ballistic limit, beyond which the delamination area decreased with increasing impact velocity.

In the following, an experimental program has been conducted to manufacture and characterize different thicknesses of kevlar/epoxy and S-2 glass/epoxy composites, and to test these composites by impacting them using small caliber projectiles. An analytical model describing the penetration of a composite target by a small caliber projectile is also presented. This model uses the circumferential strain as a failure criterion for a composite target [1]. Main assumptions are introduced and main equations representing the analytical model are presented. Representative samples of experimental results and corresponding model predictions are presented with relevant analyses and discussions.

EXPERIMENTAL WORK

An experimental program has been conducted to study the normal perforation of a small caliber projectile into two types of 3D weave composite targets with different thicknesses, respectively. The experimental facilities of the shooting range, Chair of Weapons and Ammunition, M.T.C, were used to investigate the ballistic resistance for a set of composite targets against their penetration by small caliber projectiles. In general, the scheme of the experimental work includes the following activities: (a) Choice of fabric materials and preparation of their composites, (b) characterization of prepared composites, (c) ballistic tests and measurements, and (d) post-firing examinations.

Choice of Fabric Materials and Preparation of Their Composites

3D weaveTM fabrics (kevlar-129 and S-2 glass) were selected. The reasons of this selection are: (i) the fabrics have low densities and high uni-axial tensile strengths, and (ii) the construction of fabrics enable spacing among their yarns, which permit the epoxy spreading easily in-between. Table 1 lists the data of epoxies used to manufacture each type of composite.

The main properties of kevlar-129 and S-2 glass fabrics were listed, respectively, in Table 2. The hand lay-up contact molding method was selected for manufacturing the composites (kevlar/epoxy and S-2 glass/epoxy) because: (i) it required minimum equipment, (ii) it could be used for small and large dimensions, and (iii) it produced smooth surfaces. The manufacturing process of these composites was done using the facilities of Metallurgy Dept., M.T.C., and the technological procedures were listed in Ref. [10]. Table 3 lists the main characteristics of the manufactured kevlar/epoxy and S-2 glass/epoxy composites with different thicknesses, respectively.

Characterization of Prepared Composites

Characterization of the manufactured composites was only concerned with the determination of their mechanical properties. Tensile tests were performed to determine the stress-strain behavior of

Table 1. Main data of used epoxies.

Fabric type	Epoxy base	Epoxy hardener	Mixing ratio (base: hardener)
kevlar-129	Araldite CY 219	HY 5161	2:1
S-2 glass	Araldite M	HY 956	5:1

Table 2. Properties of the used fabric types.

Fabric type	Tensile modulus [GPa]	Tensile strength [GPa]	Strain to failure [%]	Density ρ_r [kg/m ³]	Operating temp. [°C]
kevlar-129	62	3.79	3.6	1440	500
S-2 glass	85	4.8	5	2460	650

Table 3. Main characteristics of the manufactured composites.

Composite type	Number of layers, N	Thick. of composite h_c [mm]	Fiber mass, m_f [g]	Composite mass, m_c [g]	Weight fraction, W_f [%]	Density, ρ_c [kg/m ³]
kevlar/epoxy	3	3	61	110	55	883
	9	9	177	319	54.5	953
	15	15	291	510	56	982
S-2 glass/epoxy	1	4	96	192	50	1307
	3	10	283	546	51	1426
	5	15	490	938	52	1545

the manufactured composites. Standard tensile test specimens were prepared from kevlar/epoxy composite with thicknesses of 1, 3, and 6 mm, and S-2 glass/epoxy composite with thicknesses of 4, and 10 mm, respectively. Three tensile test specimens were prepared from each thickness of prepared composites.

A tensile test program was carried out on the tensile testing machine, Model MTS-810 with capacity of 100 kN, at loading rate of 50 N/sec. An extensometer was fixed on the center of the specimen gauge length. The test speed, maximum load, and other test parameters were fed to the test program. After completing the specimen failure, the obtained data points were used to draw stress-strain behavior for each specimen.

Ballistic Tests and Measurements

Ballistic tests were performed in order to determine the projectile impact and post-perforating velocities for the different thicknesses of kevlar/epoxy and S-2 glass/epoxy composite targets. The

principle of projectile velocity measurement was essentially based on measuring the time of its flight over a fixed distance (reference base). Breaking or connecting of electric circuits detected projectile arrival at a predetermined base. The measured velocity represented the velocity at the midpoint of the reference base; it was equal to the reference base divided by the measured time.

Projectile impact velocity was frequently measured at a close distance from point of impact. Because of the distance between the midpoint of reference base and target surface was small, the measured velocity was considered as the impact velocity of projectile. Projectile arrival was detected by the breaking of photocell electric circuits and the velocity measuring system displays the measuring time or projectile velocity directly on a PC screen.

The post-perforation velocity of the projectile was determined using velocity measuring frames. Each frame, which detected the projectile arrival, was connected to two-channel oscilloscope. When the projectile passed through each of the measuring frame, it connected an electric circuit and gave a signal to the oscilloscope. The time difference between the two signals was recorded and used to determine the projectile residual velocity.

The ballistic experiments were performed in the ballistic shooting range, which had provisions for the measurement of projectile impact and post-perforation velocities, respectively. The ballistic set-up mainly consists of: ballistic rifle, impact velocity and post-perforation velocity frames with their respective electronic measuring instruments, and target mount; cf. Ref. [10].

A small caliber projectile having different impact velocities was fired against each thickness of kevlar/epoxy and S-2 glass/epoxy composite targets; this velocity ranged from 200-600 m/s. The change in propellant charge mass was used to vary the projectile impact velocity. For each charge mass, a set of projectiles was fired against each tested target. Both the projectile impact and residual velocities, respectively, were measured using the velocity measuring systems used. Close measurements of minimum three shots were considered; their average represented the projectile impact velocity. In addition, the average of the corresponding measured residual velocities was evaluated and taken as the projectile residual velocity.

Post-Firing Examinations

These were mainly concerned with the arrangement and the configurations of the set up, the projectile, and the different composite targets after their perforation. After each firing test, the test set up was examined to make sure that all connections were not damaged by the projectile or by its fragments. Examining the recovered projectile after perforation of each thickness of different composite targets was very important in order to determine the degree of its deformation. This depended mainly on thickness and type of composite as well as projectile impact velocity. Each thickness of different composite targets was similarly examined in order to determine its failure mode. All interesting features related to failure mode of each thickness of different composite targets and projectiles are photographed for the analysis of test results.

ANALYTICAL MODEL

The selected analytical model that describes the penetration of a composite target by a small caliber projectile is presented herein; this model uses the circumferential strain as a failure criterion for a composite target [1]. The projectile is considered to have a diameter d_1 ($=2r_1$), and a mass m . The initial thickness of composite is denoted by h_c . In the following, the main assumptions as well as the model structure and its main equations are introduced.

Main Assumptions

- The projectile is rigid, non-deformable body, during its penetration through a composite target.
- Textile/epoxy composites are homogenous.
- The laminate consisting the composite is deformed upon impact into a conical shell with straight sides. The failure mechanism of composite is due to tensile failure of its fiber.
- The crimp force between yarns of the fabric is neglected.
- Frictions between yarns or projectile and composite are neglected.
- The epoxy is brittle and broken locally upon impact. Therefore, the projectile is assumed to penetrate the textile under the point of impact. This textile has a thickness h_c , which represents the total thickness of composite layers.

Model Structure and Main Equations

Upon the projectile impacting the fabric, a conical deformation is resulted in analogous to the V-shaped deformation. Figure 1a shows a horizontal yarn transversely impacted by projectile A traveling in the vertical direction at velocity V . Due to the impact, a longitudinal strain wave is initiated and propagated horizontally with velocity C , in opposite directions away from the impact point A. Concurrently, a transverse wave of velocity \bar{U} is generated which causes the inverted V-shaped deformation pattern to propagate to point P at time t .

The strain wave velocity C relative to such unstrained points on the yarn, at more distance away from 'C' is given by:

$$C = \sqrt{\frac{1}{M} \left(\frac{dT}{d\varepsilon} \right)_{\varepsilon=0}}, \tag{1}$$

where M is the mass per unit length of the unstrained yarn, and $(dT/d\varepsilon)_{\varepsilon=0}$ is the initial slope of the yarn tension-strain curve. The vertical velocity V and the velocity of transverse wave front \bar{U} are represented by [1]:

$$V = C \sqrt{\varepsilon(1+\varepsilon)[\sqrt{\varepsilon(1+\varepsilon)} - \varepsilon]^2}, \tag{2}$$

and

$$\bar{U} = C \sqrt{[\sqrt{\varepsilon(1+\varepsilon)} - \varepsilon]^2}, \tag{3}$$

where ε is the yarn strain. The velocity V at $\varepsilon = 0$ is represented by impact velocity V_i .

Equation (3) derived by Vinson and Zukas [4] is modified by Taylor and Vinson [1] who represented the velocity of transverse wave front as a function of projectile velocity V as:

$$\bar{U} = 64 + (0.74 \times V). \tag{4}$$

The linear conical shell theory is used to drive the equations necessary for determining the displacements, stress resultants, and couples for the generalized case of truncated conical shell under axially symmetric loading. The axial displacement of conical shell U_{tot} , at incremental time Δt is represented by (cf. Fig. 1b):

$$U_{tot} = V \Delta t = \frac{r_1 \bar{V}}{E_c h_c \sin \beta \cos^2 \beta} \ln(r_2/r_1), \tag{5}$$

where V is the projectile velocity, r_1 is projectile radius, \bar{V} is the axial load per unit of circumference, E_c is elasticity modulus of the fabric, h_c is the total thickness of the fabric, β is the rotation angle of the fabric with respect to the normal of the middle surface, and r_2 is the product of the transverse wave velocity \bar{U} and time t in addition to the radius r_1 . Equation. (5) can be used to determine the axial load \bar{V} caused when the fabric is elongated an amount U_{tot} . as follows:

$$\bar{V} = \frac{E_c h_c}{r_1} \frac{U_{tot} \sin\beta \cos^2\beta}{\ln(r_2/r_1)} \quad (6)$$

The rotational angle β is determined by:

$$\beta = \tan^{-1}(r_2/U_{tot}). \quad (7)$$

The projectile acceleration is calculated by dividing the circumferential force by the projectile mass as:

$$a_p = -2 \pi r_1 \bar{V} / m \quad (8)$$

In addition, the maximum strain at $r = r_1$ is represented by conical shell theory as:

$$\epsilon_y(r_1) = \epsilon_{y_{max}} = \frac{U_{tot} \cos\beta \sin\beta}{r_1 \ln(r_2/r_1)} \quad (9)$$

As the projectile deflects the fabric, both the level of strain and strain rate change considerably with time. Hence, the modulus of elasticity of the fabric will also change with time. From Eqn. (3) and knowing the strain of the fabric from Eqn. (9), the modulus of elasticity E_c at time t is calculated.

Input Data and Outcomes of the Present Model

The input data to the model are: (i) radius, mass and impact velocity of projectile, and (ii) strain to failure and density of a fabric material. The solution procedures of the model can be shown in Fig. 2; time is taken as an independent variable. The procedures of the solution are repeated for each incremental time Δt . The penetration process terminates when either the projectile velocity is zero, or the strain calculated using Eqn. (9) reaches the failure strain of the fabric ϵ_f , which, in turn, provides the projectile residual velocity V_r .

The model is capable of predicting the projectile residual velocity and its energy loss during penetration at each impact velocity. In addition, the time histories of the transverse wave velocity, angle of fiber, strain of fiber, modulus of elasticity, and the axial force acting on fiber during its penetration could be predicted. In the following, the predictions of the model are only concerned with the projectile velocity after perforating the different thicknesses of each composite type at each impact velocity.

RESULTS AND DISCUSSIONS

The present results are divided into: (i) characterization results of different composite materials, (ii) ballistic firing test results, (iii) comparison between ballistic resistances of largest thicknesses for tested composite targets, (iv) post-firing examinations of tested composite targets and recovered projectiles, and (v) comparison between the obtained experimental measurements and the corresponding predictions of the present model.

Characterization Results of Different Composite Materials

Figure 3 shows the stress-strain curves for kevlar/epoxy composites with thicknesses of 1, 3, and 6 mm, whereas Fig. 4 plots the stress-strain curves for S-2 glass/epoxy composites with thicknesses of 4, and 10 mm. These figures show that the values of strain to failure and tensile stress are varied with thickness of each tested composite. In addition, the relation between tensile stress and strain is non linear for each thickness of kevlar/epoxy and S-2 glass/epoxy composites. Table 4 shows the average tensile test results for each thickness of tested composites. The modulus of elasticity for each thickness of tested composites was deduced from its stress-strain behavior. A regression analysis between number of layers and corresponding strains for the tested specimens of each composite type is extrapolated to determine the failure strains of other thicknesses.

Ballistic Firing Test Results

The ballistic test results due to the impact of different thicknesses of kevlar/epoxy and S-2 glass/epoxy composite targets by a small caliber projectile having different impact velocities are presented. Symbols and digits are used to designate the tested targets; the symbols represent the kevlar/epoxy and S-2 glass/epoxy composites and the digits represent their thickness, respectively. For example, K-3 represents a kevlar/epoxy composite target with thickness of 3 mm, whereas S-10 represents a S-2 glass/epoxy composite target with thickness of 10 mm. Both the projectile velocity drop and energy loss are chosen to represent the ballistic resistance of tested composite targets to penetration.

Results for kevlar/epoxy composite targets

The obtained ballistic test results for kevlar/epoxy composite targets are used to draw the relations between the projectile residual velocity, projectile velocity drop, and projectile energy loss with impact velocity, respectively. Figure 5 depicts the change of obtained residual velocity as a function of impact velocity for different thicknesses of kevlar/epoxy composite targets. For each target thickness, the present figure shows that the residual velocity increases with impact velocity in a quasi-linear manner over the range of impact velocity used. Similar results were obtained by Cunniff [11]

Figure 6 plots the change of projectile velocity drop $\Delta V (=V_i - V_r)$ versus impact velocity for the tested kevlar/epoxy composite targets. For each target thickness, the present figure shows that the drop in projectile velocity decreases with increasing impact velocity.

The projectile energy loss ΔE is calculated as the difference between the measured projectile impact and residual energies, E_i and E_r . Figure 7 shows the change of projectile energy loss with impact velocity for different thicknesses of kevlar/epoxy composite targets. For each target thickness, it is clear from the figure that the projectile energy loss increases with impact velocity. However, the energy loss in K-3 target is approximately constant at the highest impact velocities used. The obtained trends may be attributed to that no change occurs in the failure mechanism of the tested targets, and to the strain rate of fabric, which increases with impact velocity.

Results for S-2 glass/epoxy composite targets

Figure 8 depicts the change of projectile residual velocity with impact velocity for different thicknesses of S-2 glass/epoxy composite targets. Similar to the ballistic test results of kevlar/epoxy composite, the present figure shows that the residual velocity increases with impact velocity in a quasi-linear manner. Moreover, the residual velocity of a S-10 target at $V_i = 251$ m/s is equal to zero; it means that this impact velocity represents the ballistic limit of such target thickness. Moreover, the ballistic limit of S-15 target is 395 m/s.

Table 4. Tensile test results for the different thicknesses of kevlar/epoxy S-2 glass/epoxy composites, respectively.

Material	No. of Layer N	Thick., h _c [mm]	Strain to failure, E _f [%]	Tensile stress, σ [MPa]	Elasticity modulus, E _c [GPa]
kevlar/epoxy Composite	1	1	2.2	227	10.3
	3	3	2.9	272	9.4
	6	6	3.1	375	12.1
S-2 glass/epoxy composite	1	4	2.5	181	7.2
	3	10	4.4	288	6.7

Figure 9 plots the change of projectile velocity drop with impact velocity for S-2 glass/epoxy targets. For each target thickness except for S-10 target, it is seen from the figure that the velocity drop always decreases with increasing impact velocity. In other words, the impulse transferred to target thickness decreases with increasing impact velocity. For S-10 target, the velocity drop increases beyond the ballistic limit then decreases with increasing impact velocity; this is questionable. The obtained results indicate that no change occurs in failure mechanism of such targets.

Figure 10 shows the relation between the projectile energy loss and impact velocity for tested S-2 glass/epoxy composite targets. It is seen from the figure that the projectile energy loss is direct proportional to impact velocity and target thickness. For each target thickness, the projectile dissipates its lowest energy at its lowest impact velocity. Therefore, the ballistic resistance of the target to penetration increases with the impact velocity; this is attributed to the increase of strain rate of glass fiber with impact velocity.

Comparison Between Ballistic Resistances of Largest Thickness for Tested Composite Targets

Figure 11 depicts the velocity drop ratio versus impact velocity for the largest thicknesses of different tested targets, i.e. K-15 and S-15 composite targets. For each target, the projectile velocity drop ratio decreases with increasing projectile impact velocity. Moreover, it is seen from the figure that the ballistic resistance of S-15 target is greater than that of K-15 target. At V_i = 570 m/s, the projectile velocity drop ratio decreases by 58.9 % due to perforation of S-15 target, whereas the velocity drop ratio decreases by 22.4 % due to perforation of K-15 target.

Figure 12 plots the energy loss ratio versus impact velocity for the largest target thicknesses of different tested composite targets. The change of energy loss ratio with impact velocity gives similar trends as that of Fig. 11. Moreover, the projectile dissipates 83% of its impact kinetic energy in perforating the S-15 target at V_i = 570 m/s, whereas the corresponding energy loss ratio for K-15 target is 20%.

From the ballistic test results of the tested composite targets, it can deduce that:

- The ballistic resistance of kevlar/epoxy composite targets is limited and it cannot defeat the used projectile alone over the used range of impact velocity.
- A great number of layers of kevlar/epoxy composites are needed to stop the used projectile, which, in turn, increases the mass of required target.

- The ballistic resistance of S-2 glass/epoxy targets is relatively good in comparison with that of kevlar/epoxy tested targets over the used range of impact velocity.
- A small increase in the largest thickness of tested S-2 glass/epoxy target is needed to defeat the projectile at $V_i = 570$ m/s.
- The S-15 target defeats the projectile at $V_i = 395$ m/s. The areal density of such a target is 21.6 kg/m^2 .

Post-Firing Examinations

In the following, samples of the post-firing examination results are presented for recovered projectiles and tested composite targets, respectively.

For kevlar/epoxy composite targets

The recovered projectiles after perforating the kevlar/epoxy composite targets are inspected. These projectiles are not subjected to considerable changes in their shapes. Figure 13 shows a group of recovered projectiles after perforating K-9 targets at impact velocities ranged from 400 - 500 m/s.

Figure 14 shows a photograph for the back face of a K-9 tested target. It is seen from this figure that this target is always failed by tensile failure. The yarns of the fabric are subjected to high strains due to projectile penetration and the strains of the stretched yarns reach their failure value. Also, the damage area during the penetration process is localized, which is the main advantage of the used epoxy with the tested kevlar-129 fabric.

For S-2 glass/epoxy composite targets

Figure 15 shows a recovered projectile after perforating a S-10 target at $V_i = 375$ m/s. It is clear from the figure that the target strongly resists the impacted projectile and subjects it to a significant deformation.

Figure 16 shows a photograph for the back face of a S-10 target after impacting it with different velocities. It is seen from the photograph that the projectile is trapped at $V_i = 251$ m/s. In addition, the failure mode of this target is always tensile failure, associated with a small delamination between layers. The yarns of the fabric are exposed to high strain during the penetration process. The strain of the stretched yarns reaches to their strain to failure value and the yarns protrude from the back face of the target. The damage in the perforated area is localized; the damaged area in this target is greater than that of kevlar/epoxy target with the same thickness which subjects to the same impact conditions.

Comparison between Measured and Predicted Results

In the following, the experimental measurements obtained due to the impact of different thicknesses of each tested composite target by a small caliber projectile having different impact velocities are compared with the predictions of the analytical model. Moreover, the relative differences between the measured and predicted results are calculated. The present model is run to predict the projectile residual velocities after perforating the kevlar/epoxy and S-2 glass/epoxy composite targets with different thicknesses due to their impact by a projectile with different velocities used. Projectile mass and its radius are fed to the program, whereas the data of each tested composite target that fed to the program are listed in Table 5.

Figure 17 shows the predicted change of projectile residual velocity with impact velocity for different thickness of kevlar/epoxy composite targets. For each target thickness, the measured residual velocities corresponding to different impact velocities are also depicted on the same figure. Good agreement is obtained between measured and predicted residual velocities over the used range of

Table 5. Input data of composite targets necessary to run the present analytical model.

Material	Parameter	Target designation		
		K-3	K-9	K-15
Kevlar/epoxy Composite	Density of Fabric, ρ_f [kg/m ³]	1440		
	Thickness h_c [mm]	3	9	15
	Strain to failure, ϵ_f [%]	2.9	3.3	3.6
Material	Parameter	Target designation		
		S-4	S-10	S-15
S-2 glass/epoxy Composite	Density of Fabric, ρ_f [kg/m ³]	2460		
	Thickness h_c [mm]	4	10	15
	Strain to failure, ϵ_f [%]	2.5	4.4	6.34

impact velocity. In addition, the model predicts the ballistic limits for K-3, K-9 and K-15 targets; these are 60, 140 and 230 m/s, respectively.

The maximum relative differences between the measured and predicted residual velocities for each thickness of kevlar/epoxy composite targets results are associated with the lowest impact velocities used; this may be attributed to the delamination effect between the target layers which is not considered in the present model. The maximum relative differences between predicted and measured residual velocities are found to be 16.8 % for a K-3 target at $V_i = 220$ m/s, 22.4 % for a K-9 target at $V_i = 224$ m/s, and 14 % for a K-15 target at $V_i = 240$ m/s.

Figure 18 plots the predicted change of projectile residual velocity with impact velocity for different thicknesses of S-2 glass/epoxy composite targets. Moreover, the corresponding experimental measurements are depicted on the same figure. Comparison between measured and predicted residual velocities for each target thickness proves the importance of inserting the delamination effect between layers in the present model. This may improve the predictions of the model over the lowest range of impact velocities used.

For each S-2 glass/epoxy target thickness, it is seen from the Fig. 18 that the predicted results are in good agreement with the corresponding experimental measurements for the highest three impact velocities used. In addition, the maximum differences between predicted and measured residual velocities are found to be 15.2 % for S-4 target at $V_i = 237$ m/s, 16.2 % for S-10 target at $V_i = 421$ m/s, and 8.1 % for S-15 target at $V_i = 509$ m/s. At lowest impact velocities, the relative differences between predicted and measured residual velocities for each target thickness increases.

CONCLUSIONS

- The ballistic resistance of the tested kevlar/epoxy composite targets with different thicknesses is limited. a great number of target layers is needed to stop the projectile with the highest impact velocity used which, in turn, increases the target mass.
- The amount of absorbed energy increases with increasing the target thickness and impact velocity for both kevlar/epoxy and S-2 glass/epoxy composite targets. In addition, the S-15

target is capable of defeating the used projectile at $V_i=395$ m/s; the areal density of such a target is 21.6 kg/m².

- The post-firing examination for all tested targets and their recovered projectiles show that: (i) the deformation of the projectiles that perforate the K-3 and K-9 targets is insignificant. However, the projectile is subjected to a considerable deformation when it perforates a K-15 and different thicknesses of S-2 glass/epoxy targets, (ii) yarns of kevlar and S-2 glass fabrics are subjected to high strain and failed by tension, (iii) the damaged areas in kevlar/epoxy and S-2 glass/epoxy composite targets are localized, and (iv) the delamination between composite layers is significant at the lowest impact velocities used.
- For each tested composite target, the projectiles residual velocities are compared with that of the corresponding predictions of the present analytical model; good agreement is generally obtained. Moreover, the maximum relative difference between the measured and predicted residual velocities is found to be 22.4 % at $V_i= 224$ m/sec for the K-9 target.
- The maximum relative differences between the measured and predicted results for each target thickness are found at the lowest impact velocities used, this may be attributed to the effect of the delamination between the composite layers which is not considered in the analytical mode of the present work.

REFERENCES

1. Taylor, W. A. and Vinson, J. R., "Modeling Ballistic Impact into Flexible Materials", J. AIAA, Vol. 28, No. 12, pp. (1992)
2. Waclawik, S., "Technology and Design Trends in U.S. Army Body Armor Board", Personal Armor System Symp. [PASS 98], Colchester, UK (1998).
3. Mohamed, M. H., Bogdanovich, A. E., Dicknison, L. C., Singletary, J. N. AND Lienhart, R. B., "A New Generation of 3D Woven Fabric Performs and Composites", Courtesy of the SAMPE J., Vol. 37, No. 3, pp. 8-17 (2001).
4. Vinson, J. R. and Zukas, J. A., "On the Ballistic Impact of Textile Body Armor", J. Appl. Mech., Vol. 42, pp. 263-268 (1975).
5. Zhu, G., Goldsmith, W. and Dharan, C. K., "Penetration of Laminated Kevlar by Projectiles-II. Analytical Model", Int. J. Solid Struct., Vol. 29, No.4, pp. 421-436 (1992).
6. Morye, S. S., Hine, P. J., Duckett, R. A., Carr, D. J. and Ward, I. M. 'Modelling of the Energy Absorption by Polymer Composites upon Ballistic Impact', Personal Armor System Symp. [PASS 98], Colchester, UK (1998).
7. Sharma, N., Kelly, P., Carr, D. and Viney, C., "Modeling the Ballistic Performance of Body Armor Using a Finite Difference Code", Dep. of Materials, Oxford University, (DCTA), Ministry of Defense, U.K. (1998).
8. Shahkarami, A., William, K., Vaziri, A., Poursartip, A. and Pageau, G., "Numerical Modeling of the Ballistic Response of Textile Materials", Defense Research Establishment Valcartier, University of British Columbia, Canada (1998).
9. Potti, S. V. and Sun, C. T., "Prediction of Impact Induced Penetration and Delamination in Thick Composite Laminates", Int. J. Impact Engng. ,Vol. 19, No. 1, pp. 31-48 (1997).
10. Salah, S. A., "Ballistic Resistance of Selected Composites and Textiles", M. Sc. Thesis, M.T.C., Cairo, Egypt (2002).
11. Cunniff, P. M., "An Analysis of the System Effects in Woven Fabrics under Ballistic Impact", J. Textile Res., Vol. 62, No.9, pp. 495-509 (1992).

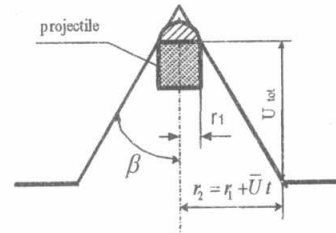
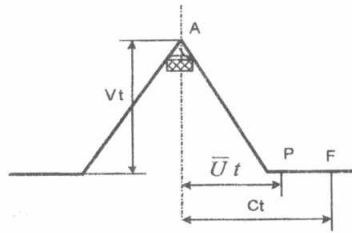


Fig. 1a. Horizontal yam impacted by projectile [1].

Fig. 1b. A schematic of impacted textile fabric [1].

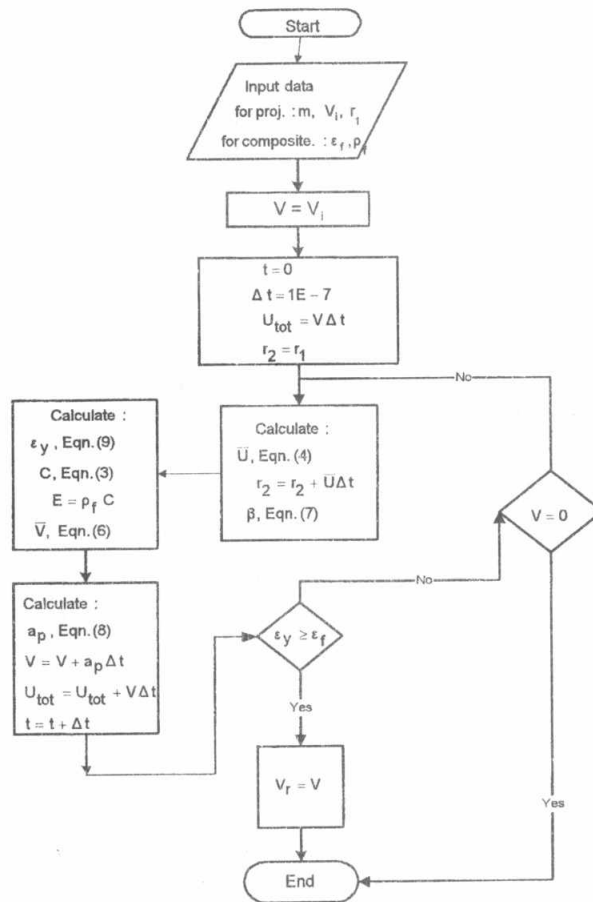


Fig. 2. Flow chart showing the procedures of solution for a composite target.

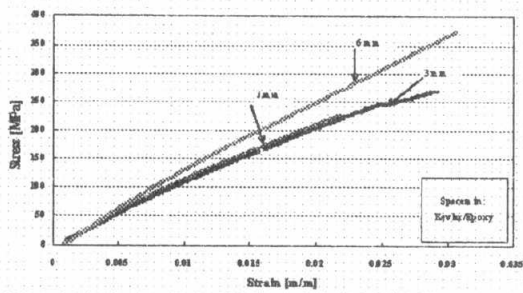


Fig. 3. Stress-strain curves for kevlar/Epoxy composites with thicknesses of 1, 3 and 6 mm, respectively.

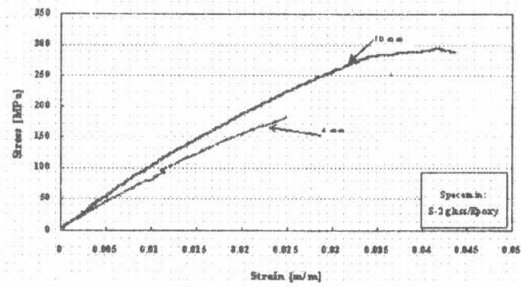


Fig. 4. Stress-strain curves for S-2 glass/Epoxy composites with thicknesses of 4, and 10 mm, respectively.

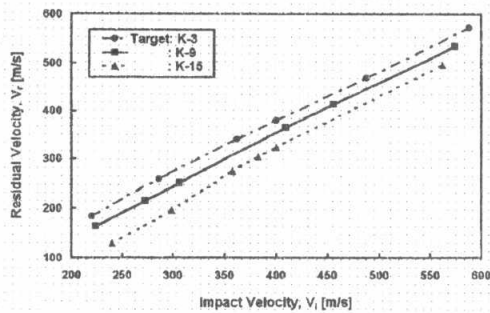


Fig. 5. Measured residual velocity versus impact velocity for different thicknesses of kevlar/epoxy composite targets.

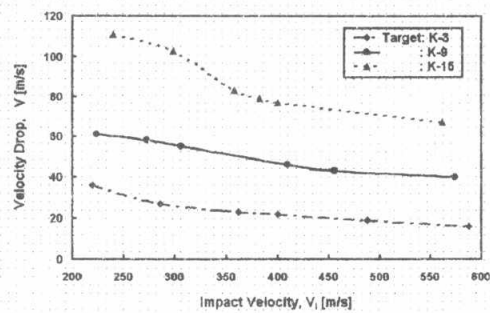


Fig. 6. Projectile velocity drop versus impact velocity for different thicknesses of kevlar/epoxy composite targets.

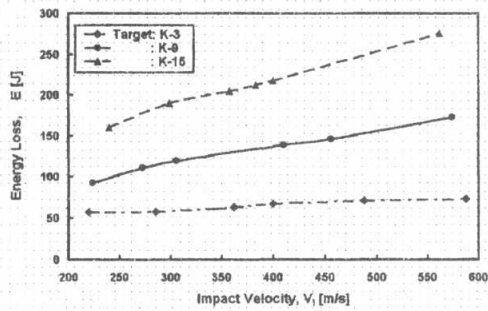


Fig. 7. Projectile energy loss versus impact velocity for kevlar/epoxy composite targets.

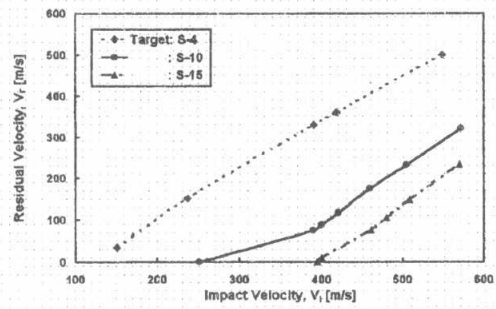


Fig. 8. Measured residual velocity versus impact velocity for different thicknesses of S-2 glass/epoxy composite targets.

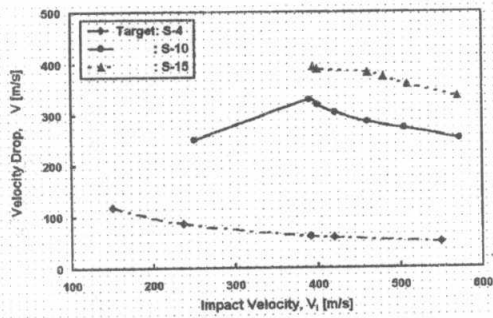


Fig. 9. Projectile velocity drop versus impact velocity for different thicknesses of S-2 glass/epoxy composite targets.

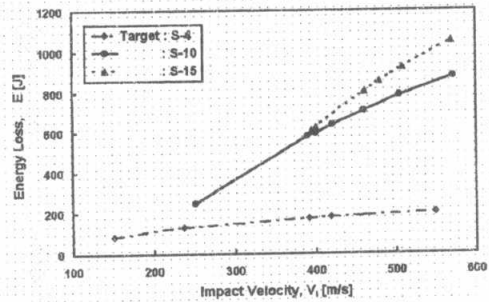


Fig. 10. Projectile energy loss versus impact velocity for S-2 glass/epoxy composite targets.

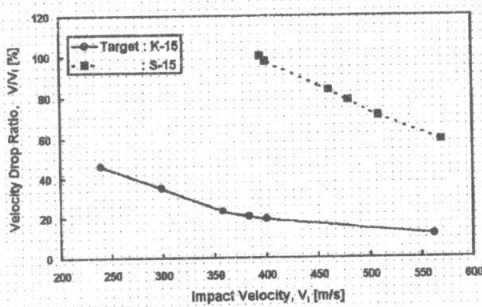


Fig. 11. Velocity drop ratio as function of impact velocity for largest thickness of tested targets.

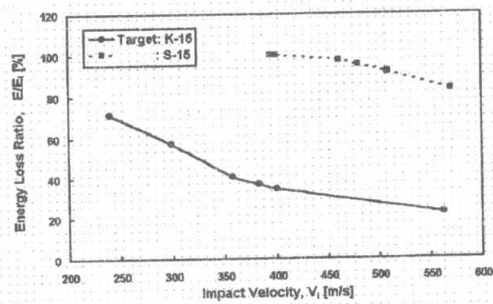


Fig. 12. Energy loss ratio as function of impact velocity for largest thickness of tested targets.

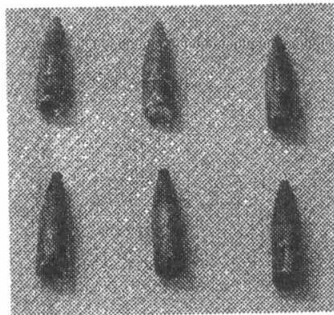


Fig. 13. Recovered projectiles after perforating K-9 target with impact velocity ranged from 400-500 m/s.

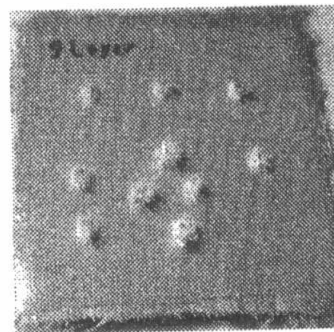


Fig. 14. Back face of a K-9 target showing tensile failure mode.

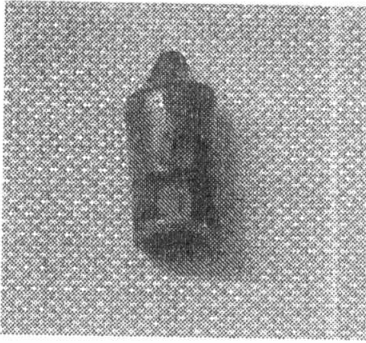


Fig. 15. A Recovered projectile after perforating S-10 target with $V_i = 375$ m/s.

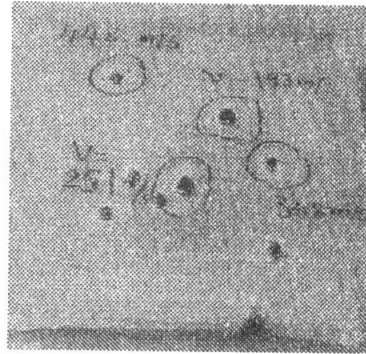


Fig. 16. Front face of a S-10 target showing projectile trap at $V_i = 251$ m/s.

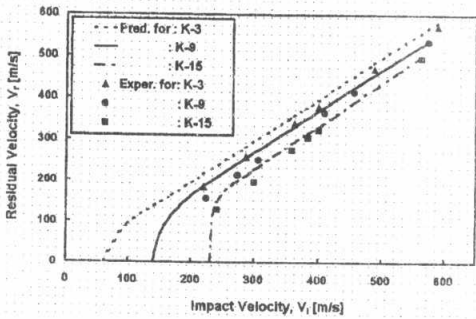


Fig. 17. Comparison between predicted and measured residual velocities for different thickness of kevlar/epoxy composite targets.

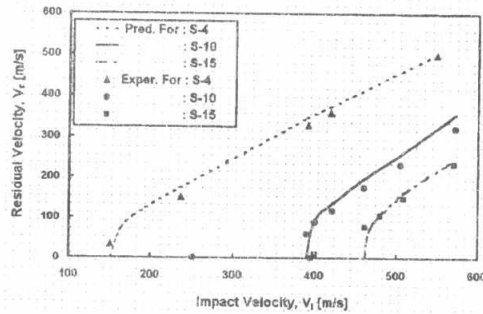


Fig. 18. Comparison between predicted and measured residual velocities for different thickness of S-2 glass/epoxy composite targets.